JACS
JOURNAL OF THE AMERICAN CHEMICAL SOCIETY

Article

pubs.acs.org/JACS

Thermodynamics of HIV-1 Reverse Transcriptase in Action Elucidates the Mechanism of Action of Non-Nucleoside Inhibitors

Guillaume Bec,[†,⊥] Benoit Meyer,[†,⊥] Marie-Aline Gerard,[†,§] Jessica Steger,[‡,∥] Katja Fauster,[‡] Philippe Wolff,[†] Dominique Burnouf,[†] Ronald Micura,[‡] Philippe Dumas,[†] and Eric Ennifar*[,†]

[†]Architecture et Réactivité des ARN, CNRS/Université de Strasbourg, Institut de Biologie Moléculaire et Cellulaire, 15 rue René Descartes, 67084 Strasbourg, France

[‡]Institute of Organic Chemistry, Center for Molecular Biosciences Innsbruck (CMBI), University of Innsbruck, 6020 Innsbruck, Austria

Supporting Information

ABSTRACT: HIV-1 reverse transcriptase (RT) is a heterodimeric enzyme that converts the genomic viral RNA into proviral DNA. Despite intensive biochemical and structural studies, direct thermodynamic data regarding RT interactions with its substrates are still lacking. Here we addressed the mechanism of action of RT and of non-nucleoside RT inhibitors (NNRTIs) by isothermal titration calorimetry (ITC). Using a new incremental-ITC approach, a step-by-step thermodynamic dissection of the RT polymerization activity showed that most of the driving force for DNA synthesis is provided by initial dNTP binding. Surprisingly, thermodynamic and kinetic data led to a reinterpretation of the mechanism of inhibition of NNRTIs. Binding of NNRTIs to preformed RT/DNA complexes is hindered by a kinetic barrier and NNRTIs mostly interact with free RT. Once formed, RT/NNRTI complexes bind DNA either in a seemingly polymerase-competent orientation or form high-affinity dead-end complexes, both RT/NNRTI/DNA complexes being unable to bind the incoming nucleotide substrate.

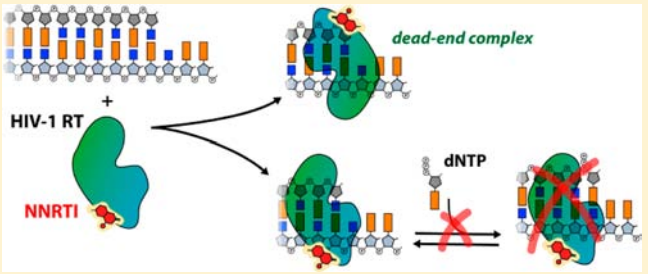

INTRODUCTION

HIV-1 reverse transcriptase (RT) is a multifunctional enzyme that converts the genomic HIV RNA into proviral DNA by catalyzing RNA- and DNA-dependent DNA polymerase reactions in addition to a ribonuclease H (RNase H) activity. RT is an asymmetric heterodimer composed of p66 and p51 subunits, both produced by the cleavage of the Gag-Pol polyprotein by the viral protease. The p66 subunit contains both enzymatic active sites comprised of a polymerization and an RNase H domain.[1,2] It contains four subdomains termed "fingers", "palm", "thumb", and "connection" by analogy to a right hand. To date, RT remains an important target for antiretroviral therapy since half of the 26 individual agents licensed for the treatment of HIV-1 infection target the RT polymerization activity. These drugs are divided into two classes: (i) nucleoside- and nucleotide-analogue RT inhibitors (NRTIs), which compete with the natural nucleoside substrate and act as terminators of DNA synthesis after incorporation into the primer strand, and (ii) non-nucleoside RT inhibitors (NNRTIs). Five NNRTIs have been approved for clinical use by the U.S. Food and Drug Administration: nevirapine, delviradine, efavirenz, etravirine (TMC 125), and, more recently, rilpivirine (TMC 278). As revealed by numerous crystal structures, all NNRTIs target the same hydrophobic pocket (non-nucleoside inhibitor binding pocket, NNIBP) located in the palm domain of the p66 subunit about 10 Å from the polymerase catalytic site.[2−6]

Steady-state and presteady-state kinetic analyses have been used to elucidate the mechanism of action of various NNRTIs,[7−9] suggesting that their interaction with RT does not prevent the dNTP substrate binding but rather dramatically reduces the rate of dNTP incorporation by interfering with the chemical step of DNA synthesis. However, recent studies performed using biophysical approaches have shown that the precise inhibition mechanism is still ambiguous. For example, a recent crystal structure of a RT/DNA/nevirapine complex revealed that the dNTP binding pocket is distorted in presence of the inhibitor, shifting the 3′-end of the DNA primer away from the polymerase active site,[10] casting doubt on the ability of RT to bind dNTP in this state. In addition, single-molecule FRET (smFRET) assays showed that RT can slide between opposite termini on long duplexes and rapidly switches between two orientations (polymerization- or RNaseH-competent modes) when it binds polypurine RNA sequences that are primers for plus-strand synthesis. Flipping and sliding kinetics are modulated by binding of incoming dNTP and NNRTIs, which stabilize and destabilize the polymerization-competent orientation, respectively.[11,12]

Received: February 20, 2013
Published: June 6, 2013

   dx.doi.org/10.1021/ja4018418 | J. Am. Chem. Soc. 2013, 135, 9743−9752

The enzymatic activities of RT and mechanisms of inhibition by RT inhibitors have been intensively investigated using biochemical and structural approaches over the past 30 years. Several advanced biophysical approaches, such as surface plasmon resonance,[13−16] single molecule techniques,[11,12,17,18] or mass spectrometry[19] provided significant and complementary insights into the understanding of various processes involving RT. However, somewhat surprisingly, thermodynamic data regarding RT interactions are still lacking. When integrated with other experimental methodologies, thermodynamic data are essential for a complete description of any binding interaction, revealing forces driving complex formation and providing insights into mechanisms of action. Thermodynamic data are also essential for linking structural data with *in silico* modeling. In this study we report a detailed thermodynamic study of DNA polymerization by RT and of the mechanism of inhibition of NNRTIs using isothermal titration calorimetry (ITC). ITC is a label-free and true in-solution technique and is considered the "gold standard" assay for binding since it directly provides, in one single experiment, the complete binding profile between two molecules (binding affinity, enthalpy and entropy changes, stoichiometry).[20−23] Using a novel "incremental ITC" strategy, the mechanism of DNA polymerization by RT was dissected step by step through successive additions in the ITC cell of consecutive RT substrates. We showed that, by providing a free-energy change almost similar to that of dNTP hydrolysis, the initial binding step of an incoming dNTP provides much of the driving force for DNA synthesis. Interactions between NNRTIs and RT or RT/DNA complex were also dissected thermodynamically. A joint processing of the titration curves at different temperatures together with a kinetic parameter determination was performed using the kinITC approach recently developed in our laboratory.[24] Unexpectedly, our results clearly show that the incoming nucleotide is unable to bind the RT/DNA complex in presence of NNRTI, in contradiction to the current model of NNRTI inhibition. In view of these results, we propose a reinterpretation of the mechanism of inhibition of NNRTIs highlighting two inhibition pathways. Consequences for the inhibition of RT by NNRTI *in vivo* are discussed.

RESULTS

Analysis of RT Binding to a DNA Primer-Template. The first step in DNA polymerization involves binding of RT to a DNA primer-template. Using ITC microcalorimetry, we first investigated the binding of RT to a 20-/27-mer primer-template over the 5−30 °C temperature range (Figures S1 and S2). Our data (Table 1 and Figure 1) show that the RT-DNA interaction is endothermic ($\Delta H > 0$) in this temperature range, with an affinity in the low nanomolar range, in agreement with available biochemical data.[25,26] The binding is therefore entropy driven, which might result from the predominance of minor groove over major groove interactions, leading to the displacement of ordered cations and water molecules from DNA by positively charged protein residues.[22,27] A comparison with thermodynamic parameters of DNA binding by Taq and Klenow polymerases[28,29] shows a similar affinity of all three enzymes for DNA. However, the entropic contribution to DNA binding is significantly more favorable in the case of RT, possibly due to the additional interactions provided by the RNaseH domain and the p51 subunit with the DNA minor groove.[30]

Table 1. Thermodynamics of RT/DNA Binding[a]

temp (°C)	ΔH (kcal·mol^{-1})	$-T\Delta S$ (kcal·mol^{-1})	K_d (nM)
5[b]	28.9 ± 0.9	−38.0 ± 1.0	70 ± 2
10[c]	25.2 ± 1.8	−34.5 ± 1.7	60 ± 3
15[b]	20.4 ± 1.9	−30.1 ± 1.8	48 ± 4
20[d]	16.1 ± 0.1	−26.0 ± 0.2	41 ± 4
25[c]	10.4 ± 0.1	−20.5 ± 0.1	38 ± 2
30[c]	4.7 ± 0.2	ND	ND

[a]All data were obtained on a ODN20/MATODN27A DNA primer-template. ND denotes "not determinable" since the Wiseman parameter c is >1000. [b]Average values and standard deviations of two independent experiments. [c]Average values and standard deviations of three independent experiments. [d]Average values and standard deviations of four independent experiments.

Interestingly, using our 20-/27-mer DNA sequence, only one binding configuration was observed (except at 5 °C where a minor secondary binding mode was also observed as shown in Figure S2), presumably the polymerization competent one according to the following experiments. However, for different primer-template sequences, two major modes of interactions were observed (Figure S3), in agreement with single molecules studies of RT/nucleic acid substrates.[11,12,18] Analysis of the temperature dependence of the binding enthalpy $\Delta C_p = \partial \Delta H/\partial T$ (Figure 1b) reveals a large, nonconstant, negative heat capacity change (ΔC_p ranging from −0.74 to −1.14 kcal·mol^{-1}·K^{-1} between 5 and 30 °C), similar to the one observed for the Taq DNA polymerase (−0.73 kcal·mol^{-1}·K^{-1})[28] and for the Klenow fragment (−0.87 to −0.97 kcal·mol^{-1}·K^{-1}).[29] Because of this large negative heat capacity change, which is usually considered a hallmark of local folding coupled to binding,[31] extrapolation of our data to higher temperatures shows that the binding enthalpy is 0 at 34 °C (Figure 1b). According to the van't Hoff equation $(\partial \ln K_d/\partial T) = -\Delta H/(RT^2)$, a null ΔH implies that the binding affinity is at an extremum at that temperature, which turns out to be a maximum due to the sign of ΔC_p. Consequently, the optimal DNA binding affinity is close to the physiological temperature for the virus.

Following RT Polymerization Step by Step Using Incremental ITC. In order to follow each step of DNA elongation, we set up a novel 'incremental-ITC' protocol which enables one to monitor successive chemical reactions in the sample cell (Figure 2 and Figure S4). After the addition of DNA into protein in a first ITC experiment, the content of the cell is kept and the syringe is reloaded with the first incoming nucleotide substrate. The first round of polymerization is then followed by running another ITC experiment. After completion of this reaction, the syringe is loaded again with the second incoming nucleotide substrate (that should be different from the previous one) and a third successive ITC experiment is performed on the same sample to perform a second round of polymerization. Using this strategy, we could follow up to five consecutive reactions, including the addition of all four dNTPs.

By using natural dNTP nucleotides, one can only observe a complete round of polymerization (i.e., initial dNTP binding, chemical step, and translocation). However, by first incorporating a dideoxynucleotide (ddNTP) into the primer strand, further nucleotide incorporation is prevented, which allows one to observe the contribution of initial dNTP binding alone in absence of catalysis (Figure 2, ddATP is used in the fourth ITC experiment, and dGTP initial binding was thus observed in the

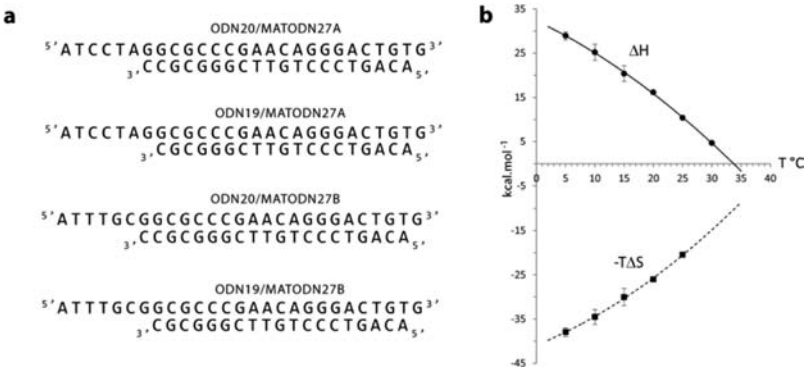

Figure 1. Thermodynamics of RT binding to a DNA primer-template. (a) Sequences of DNA primer-templates used in this study. (b) Temperature dependence of ΔH and $-T\Delta S$ for RT binding to a DNA primer-template ODN19/MATODN27B. The curves are merely the result of a quadratic fit. At 30 °C, where the Wieseman parameter c is >1000, only the binding enthalpy could be accurately determined.

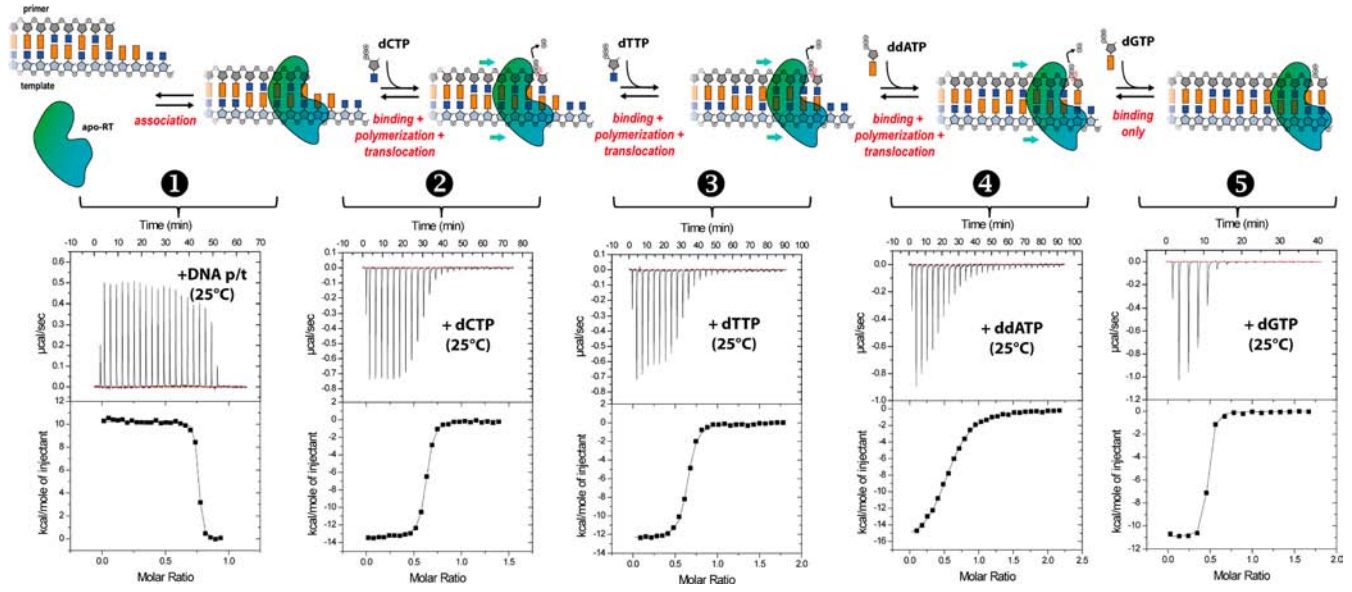

Figure 2. Example of incremental-ITC experiment. Five successive experiments were performed at 25 °C on the same sample: addition of (1) DNA primer-template ODN19/MATODN27B (560 μM) into RT (60 μM in the ITC cell), followed by sequential injection of the incoming nucleotides (2) dCTP, (3) dTTP, (4) ddATP, and (5) dGTP (900 μM).

fifth ITC experiment). Using this approach, it is therefore possible to obtain the thermodynamic parameters both of overall nucleotide incorporation reaction (ΔH_{pol}, ΔS_{pol}, and ΔG_{pol}) and of nucleotide binding only (ΔH_{bind}, ΔG_{bind}, and ΔS_{bind}). Importantly, the difference between these two sets of terms yields the thermodynamic parameters for the chemical reaction and the protein translocation (which are inextricable in our experiments):

$$\Delta H_{cstr} = \Delta H_{pol} - \Delta H_{bind}$$

$$\Delta S_{cstr} = \Delta S_{pol} - \Delta S_{bind}$$

$$\Delta G_{cstr} = \Delta G_{pol} - \Delta G_{bind}$$

Incorporation of nucleotides into the DNA template following incremental-ITC experiments was assessed by mass spectrometry analysis (Figure S5).

Following formation of the RT/DNA primer-template complex, series of incremental-ITC experiments were performed with successive additions of dTTP and dATP (Figure S6), ddTTP and dATP (Figure S7), dTTP, ddATP and dGTP (Figure S8), ddCTP and dTTP (Figure S9), and dGTP and dCTP (Figure S10). Finally, data for dCTP binding only were obtained on a ddG-terminated RT/DNA complex (Figure S11). Here, it is important to emphasize that if a reaction corresponding to the binding-only of a dNTP onto a previously incorporated ddNTP is correctly described by a dimensioned dissociation constant K_d, this is not the case with the full reaction leading to incorporation of a new nucleotide. Indeed, such a reaction amounts to

$$RT/DNA_n + dNTP \leftrightarrows RT/DNA_{n+1} + PPi$$

which, *a priori*, can only be described by a dimensionless equilibrium constant. However, we clearly established that, in our conditions, the amount of free pyrophosphate (PPi) remained sufficiently small (due to precipitation of insoluble magnesium pyrophosphate) that the latter description was not adequate, whereas an apparent dissociation constant described correctly our data (see Supporting Information).

Thermodynamic parameters were derived for dTTP, ddTTP, dATP, ddATP, dCTP, ddCTP and dGTP nucleotide incorporation and for the four natural dNTPs binding in

dx.doi.org/10.1021/ja4018418 | J. Am. Chem. Soc. 2013, 135, 9743−9752

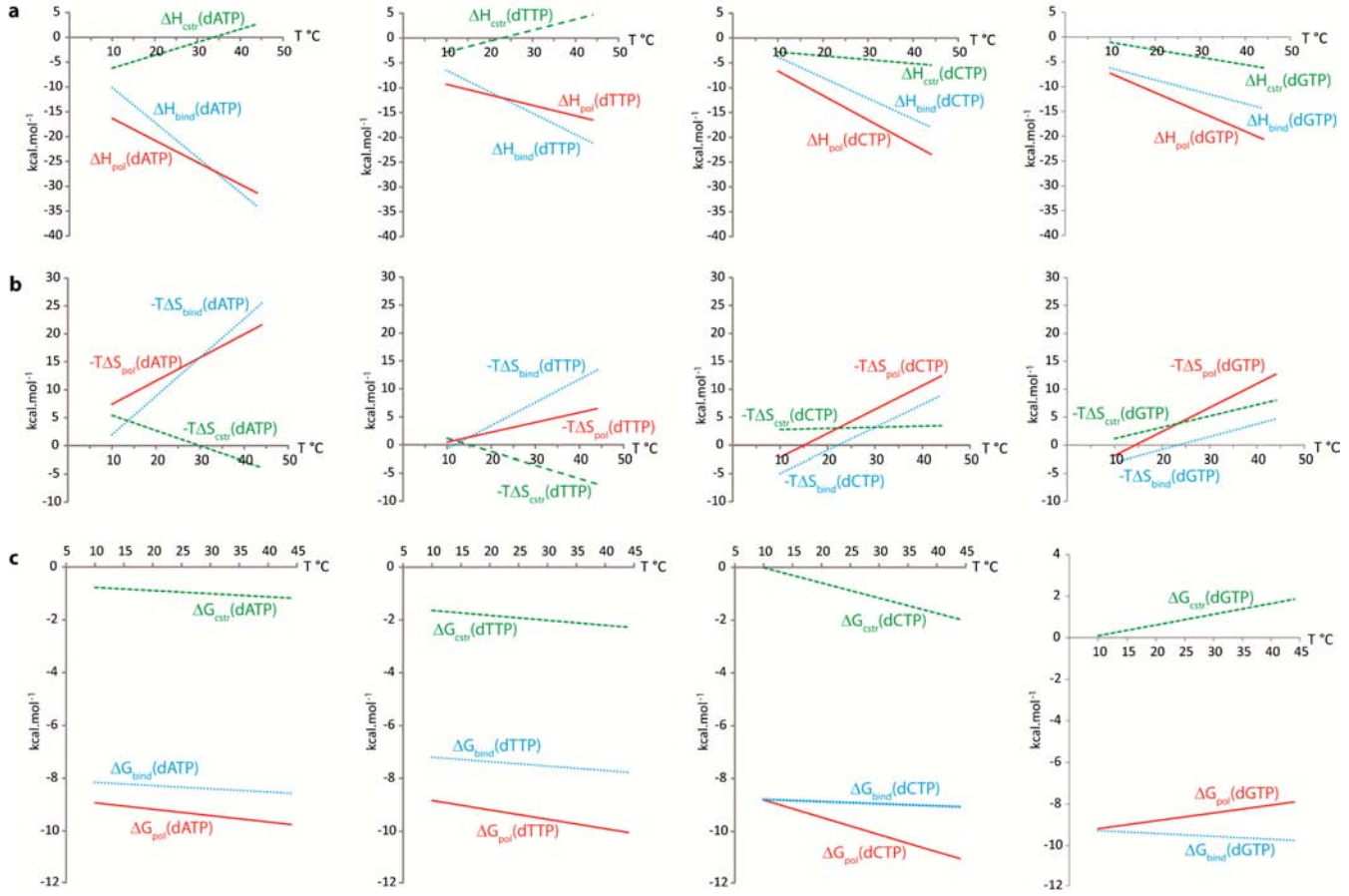

Figure 3. Thermodynamics of incoming nucleotide binding to RT/DNA complex. Temperature dependence of (a) ΔH, (b) $-T\Delta S$, and (c) ΔG are shown for incoming nucleotides dATP, dTTP, dCTP, and dGTP to the RT/DNA complex. Observed enthalpy, entropy, and Gibbs free energy changes for nucleotide initial binding only (ΔH_{bind}, $-T\Delta S_{bind}$, ΔG_{bind}) are represented with cyan dotted lines. Analogous parameters for overall nucleotide incorporation (ΔH_{pol}, $-T\Delta S_{pol}$, ΔG_{pol}) are represented with red solid bold lines. Deduced parameters for the chemical plus the translocation steps (ΔH_{cstr}, $-T\Delta S_{cstr}$, ΔG_{cstr}) are represented with green dashed lines. Experimental data are reported in Figure S12 and Tables S1 and S2 and were fitted with a linear least-squares regression.

absence of catalysis. (Figure 3, Tables S1 and S2 and Figure S12). Dissociation constants obtained by ITC are, after temperature correction, slightly lower than those obtained by biochemical approaches.[25,32,33] Quite surprisingly, the binding of dTTP is significantly weaker than those of other dNTPs (Table S2), which might reflect a possible effect of sequence context effect. Unlike the RT-DNA interaction, which is endothermic, binding of dNTP or ddNTP to RT/DNA complex is exothermic (as expected). Enthalpy changes for nucleotide incorporation (between −10 and −24 kcal·mol^{-1}) are in good agreement with thermodynamic data obtained by stopped-flow calorimetry for DNA synthesis of the Klenow fragment of *E. coli* DNA polymerase I (between −10 and −16 kcal·mol^{-1}).[34] However, in the latter study, the enthalpic contribution of initial binding of dNTP could not be observed.

To assess that ΔH_{bind} is exclusively due to initial binding of dNTP and not to a possible polymerization of nonelongated DNA after dissociation of RT from the DNA template-primer +1, a control experiment was performed using a purified ddT-terminated RT/DNA cross-linked complex[30,35] with incoming dATP. This experiment led to thermodynamic parameters for dATP binding that were remarkably similar to the results obtained with the noncovalent RT/DNA complex (Figure S13 and Table S2), thus validating the incremental-ITC strategy. We also performed control experiments with the addition of a mismatched nucleotide, which did not show any significant binding (Figure S14).

Interestingly, for 20-/27-mer DNA primer-template sequences showing only one RT binding mode, the fraction of DNA-binding competent RT correlates well with the fraction of incoming nucleotide bound or elongated. This shows that the binding orientation adopted by the RT for this DNA sequence corresponds to the polymerization-competent binding observed in crystal structures.[30,36] However, the two other DNA primer-template substrates used in our study led to two thermodynamically distinct RT binding modes, only one being catalytically competent (Figure S3). Most likely, the incompetent binding mode corresponds to an orientation of the RT where the RNaseH domain is close to the 3′-hydroxyl of the DNA template as observed by smFRET.[11,12] In the case of the two modes of interaction observed with an RNA/DNA hybrid, neither RT-RNA/DNA complex is capable of proceeding with polymerization (Figure S3), in agreement with smFRET studies.[11]

kinITC Analysis of Nevirapine Binding to Free RT and RT/DNA Primer-Template Complex. We recently examined the binding of nevirapine to free RT using our newly developed kinITC approach, which allows obtaining joint thermodynamic and kinetic data on a label-free system using ITC.[24] Data derived from kinITC have led to a determination of interaction

dx.doi.org/10.1021/ja4018418 | J. Am. Chem. Soc. 2013, 135, 9743−9752

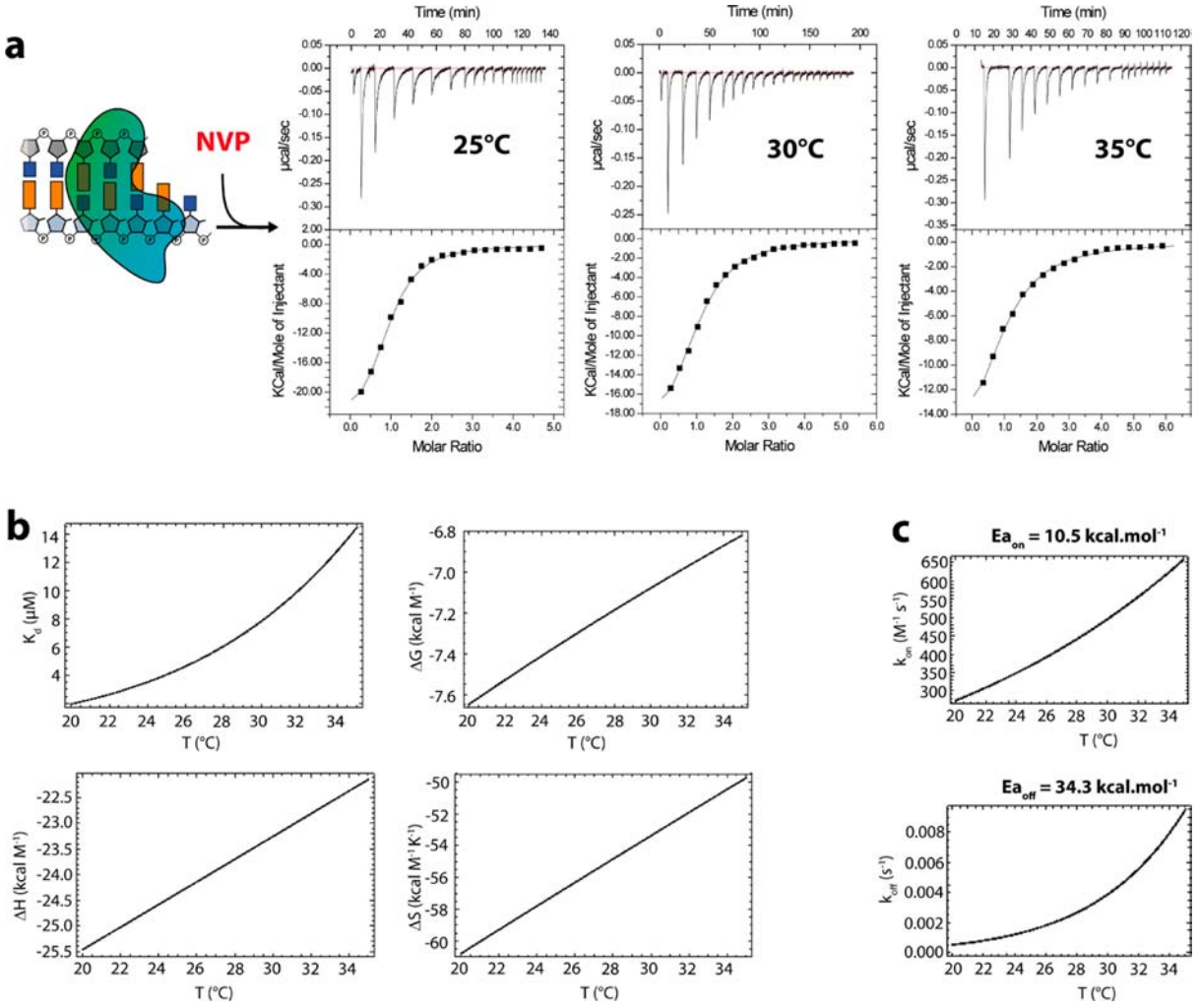

Figure 4. kinITC study of nevirapine binding to a RT/DNA primer-template complex. (a) ITC profiles at 25, 30, and 35 °C for nevirapine (546 μM in the injection syringe) binding to preincubated RT/DNA complex (22 μM in the cell, sequence ODN20/MATODN27A). (b) Thermodynamic parameters for nevirapine binding to a RT/DNA complex obtained by the 'global thermodynamic treatment' of titration curves at all temperatures. (c) Kinetic parameters k_{on} and k_{off} after fitting of the shape of all injection curves by kinITC.

kinetics in excellent agreement with surface plasmon resonance data.[13,24] Here we extended our kinITC study to the interaction of nevirapine with preincubated RT/DNA complexes. Our previous experiments performed with the 20-/27-mer DNA primer-template showed that above 5 °C, 100% of the RT/DNA complexes formed with this construct are catalytically competent. Consequently, further experiments were performed using this construct to ensure the formation of a homogeneous population of complexes. As observed from raw thermograms at 25, 30, and 35 °C (Figure 4), the binding of nevirapine to the RT/DNA complex is exceptionally slow (up to 13 min were required to ensure full return to baseline after nevirapine injection into the RT/DNA complex at 25 °C, Figures 4 and S15). Our analysis showed that the affinity of nevirapine for the RT is affected by the presence of DNA: the dissociation constant of nevirapine at 35 °C increases from 5 μM for the free RT to 14 μM for the RT/DNA complex. This change in affinity is associated with a significant decrease (4.6-fold) of the association rate constant (k_{on} = 650 M^{-1} s^{-1} at 35 °C) and a slight decrease (1.7-fold) of the dissociation rate constant (k_{off} = 9.0 × 10^{-3} s^{-1} at 35 °C) (Figure 4) as compared to the binding of nevirapine to the free RT.[24] This might be attributed to the expected reduced mobility of the enzyme in presence of DNA primer-template compared to the free enzyme, thus leading to a slower remodeling of the non-nucleoside binding pocket (which is required for nevirapine binding or dissociation). As previously observed for the RT/nevirapine interaction, the binding of nevirapine to the RT/DNA complex is associated with an anomalous positive heat capacity change ΔC_p = 0.48 kcal·mol^{-1}·K^{-1}. This most likely results from the necessary disorganization of the clathrate-like water shell around the hydrophobic nevirapine to allow its entry into the binding pocket. The nevirapine binding affinity that we observed by ITC is significantly weaker than that obtained by previous biochemical approaches (from 25 to 400 nM).[8,37] In addition to the different technique employed, these differences are likely to be due, at least partly, to variability in the lengths and sequences of DNA primer-template among these studies.[38]

Because the binding of the nucleotide substrate induces changes in the structure of the RT/DNA complex (closing of the p66 fingers subdomain on the incoming dNTP),[30,39] we also examined by ITC the binding of nevirapine onto a RT/DNA/dNTP complex. A ternary complex was obtained by mixing RT in presence of a ddT-terminated 20-/27-mer DNA primer-template and the next incoming nucleotide, dATP. ITC experiments were then performed by injection of nevirapine

dx.doi.org/10.1021/ja4018418 | J. Am. Chem. Soc. 2013, 135, 9743−9752

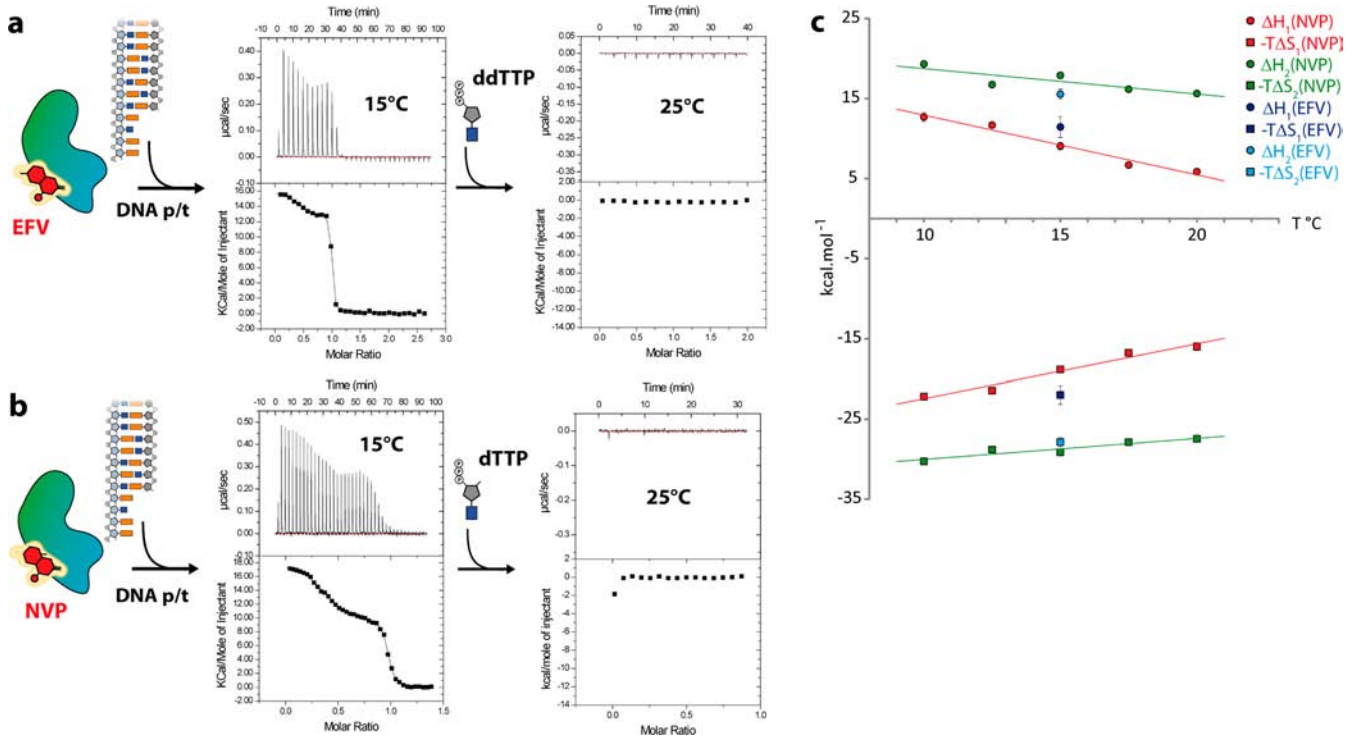

Figure 5. Thermodynamics of DNA primer-template binding to RT/NNRTI complex. (a) ITC profile at 15 °C for DNA primer-template (349 μM in the syringe, sequence ODN20/MATODN27A) binding to RT-efavirenz complex (20 μM RT and 40 μM efavirenz in the cell). The experiment was followed by the injection of ddTTP (600 μM in the injection syringe) at 25 °C. (b) ITC profile at 15 °C for DNA primer-template (295 μM in the syringe, sequence ODN20/MATODN27A) binding to preincubated RT-nevirapine complex (45 μM RT and 150 μM nevirapine in the cell). The experiment was followed by the injection of dTTP (500 μM in the injection syringe) at 25 °C. (c) Temperature dependence of ΔH (circles) and $-T\Delta S$ (squares) for DNA primer-template binding to RT/NNRTI complex. Data for RT-nevirapine complex were fitted with a linear least-squares regression.

Table 2. Thermodynamics of DNA Binding to RT/NNRTI Complex[a]

temp (°C)	N_1	ΔH_1 (kcal·mol^{-1})	$-T\Delta S_1$ (kcal·mol^{-1})	K_{d_1} (nM)	N_2	ΔH_2 (kcal·mol^{-1})	$-T\Delta S_2$ (kcal·mol^{-1})	K_{d_2} (nM)
NVP								
10	0.6 ± 0.1	12.7 ± 0.6	−22.2 ± 0.3	49 ± 25	0.3 ± 0.1	19.3 ± 0.8	−30.3 ± 0.4	4.9 ± 3.9
12.5	0.6 ± 0.1	11.7 ± 0.1	−21.5 ± 0.3	35 ± 14	0.4 ± 0.1	16.8 ± 2.2	−28.8 ± 2.0	0.5 ± 0.1
15	0.6 ± 0.1	9.1 ± 0.5	−18.9 ± 0.1	42 ± 22	0.3 ± 0.1	17.9 ± 1.1	−29.1 ± 0.9	3.4 ± 1.3
17.5	0.7 ± 0.1	6.7 ± 0.2	−16.8 ± 0.4	26 ± 12	0.3 ± 0.1	16.2 ± 0.9	−27.9 ± 0.5	1.7 ± 1.2
20	0.7 ± 0.1	5.9 ± 0.1	−16.0 ± 0.5	34 ± 32	0.3 ± 0.1	15.6 ± 0.5	−27.4 ± 1.1	2.0 ± 1.8
EFV								
15	0.5 ± 0.1	11.5 ± 1.3	−22.0 ± 1.1	10 ± 4	0.4 ± 0.1	15.5 ± 0.6	−27.9 ± 0.6	0.4 ± 0.1

[a]Average values and standard deviations of two independent experiments. All data were obtained on a ODN20/MATODN27A DNA primer-template.

aliquots into the complex. Our results showed that nevirapine is not able to bind to the RT/DNA/dNTP complex (Figure S16), likely because the NNIBP is not flexible enough within the context of the ternary complex to allow ligand entry. This result, implying that inhibition by nevirapine is not possible after the start of DNA polymerization, is potentially of great therapeutic importance.

Binding of DNA Primer-Template to RT-NNRTI Complex Leads to Two Distinct Complexes. We next investigated the thermodynamics of DNA primer-template binding to RT/NNRTI complex. In these experiments, RT (22−45 μM) was preincubated with nevirapine (3- to 7-fold excess) or efavirenz (2-fold excess). Incremental-ITC titrations were performed over the 10−20 °C temperature range for nevirapine and at 15 °C for efavirenz (Figures 5 and S17 and Table 2). We observed that, in the presence of NNRTI, RT interacts with a DNA primer-template in one of two mutually exclusive binding modes with different thermodynamic properties (sites number 1 and 2 in Table 2). The most populated (~66%) binding mode is characterized by a weakly endothermic interaction (ΔH = 6 kcal·mol^{-1} at 20 °C), and a dissociation constant of ca. 30 nM. Its heat capacity change (ΔC_p = −0.68 kcal·mol^{-1}·K^{-1}) is in the low range of the DNA binding to the free RT. In contrast, the second binding mode (~33%) is more endothermic (ΔH = 16 kcal·mol^{-1} at 20 °C), with a less negative ΔC_p (−0.37 kcal·mol^{-1}·K^{-1}) and a dissociation constant in the very low- or subnanomolar range. Based on their thermodynamic properties, both binding modes can be associated with the two types of binding obtained with 19-/32- and 26-/26-mer DNA substrates (Figure S3), i.e., a polymerization-competent orientation and an opposite orientation placing the RNaseH domain close to the 3′ end of the

dx.doi.org/10.1021/ja4018418 | J. Am. Chem. Soc. 2013, 135, 9743−9752

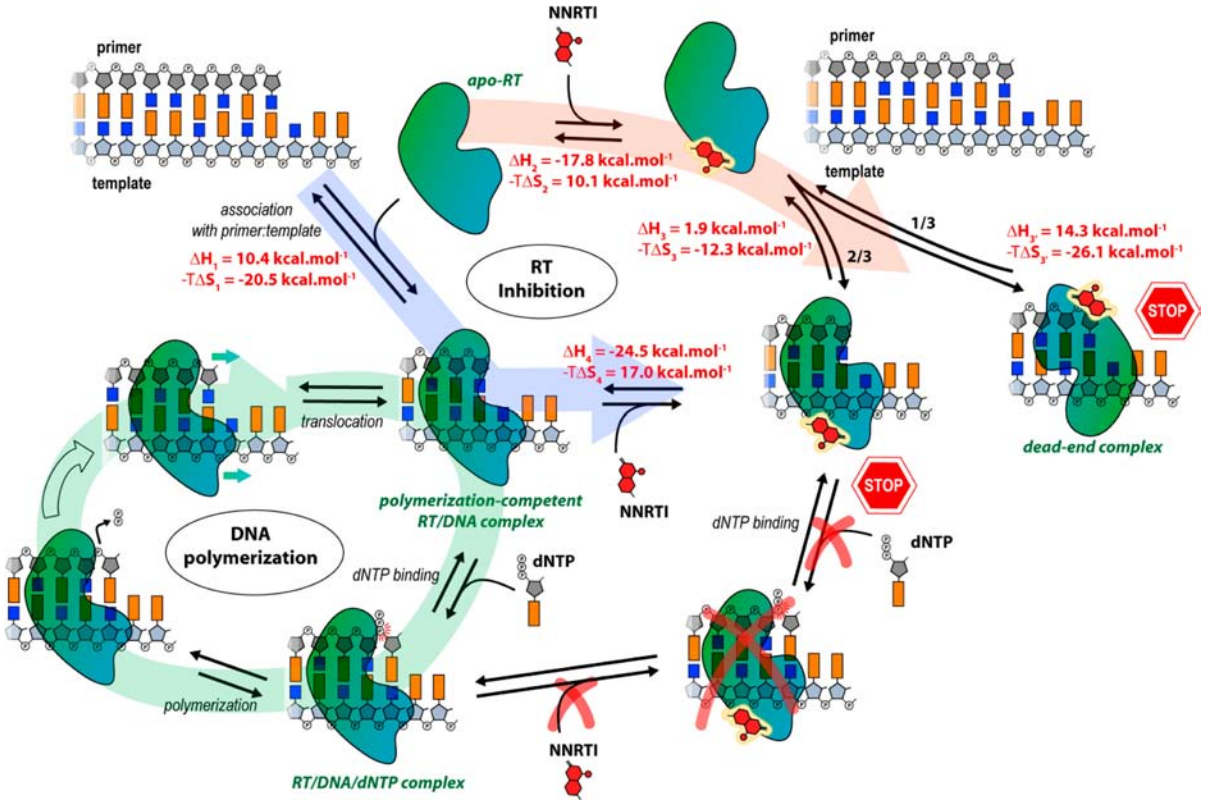

Figure 6. Mechanism of DNA polymerization by the HIV-1 reverse transcriptase and proposed inhibition mechanism for NNRTI. Variations of binding enthalpies observed at 25 °C are indicated in red. The DNA polymerization pathway is schematized on the left part of the diagram (light green). The first NNRTI inhibition pathway (light blue) involves the binding of the inhibitor to a polymerization-competent RT/DNA complex (ΔH_1, ΔS_1 and ΔH_4, ΔS_4). The second inhibition pathway (light red) involves the binding of RT to the NNRTI (ΔH_2, ΔS_2), followed by binding of the DNA primer-template. This second pathway leads to the formation of two kinds of complexes: One is a NNRTI-inhibited polymerization-competent RT/DNA complex (ΔH_3, ΔS_3), and the second one is a nonproductive dead-end complex ($\Delta H_{3'}$, $\Delta S_{3'}$). None of the RT/DNA/NNRTI complexes are able to bind the incoming dNTP substrate.

template, presumably an RNaseH-active conformation of RT. This interpretation would be consistent with previous reports showing that the polymerization-competent binding of RT onto the DNA primer-template is destabilized in favor of an RNaseH-active RT in presence of NNRTI[11,12] and by an increased RNaseH activity of RT in presence of nevirapine.[40]

Incoming Nucleotide Substrates Are Not Able to Bind the RT/DNA/NNRTI Complexes. Following addition of nevirapine to a catalytically competent RT/DNA complex (Figure 4), initial binding of the incoming nucleotide was evaluated by incremental-ITC. As seen from our previous experiments (Figure S9 and Table S2), in the absence of inhibitor, the initial binding step (without catalysis) of the incoming nucleotide (dTTP or ddTTP) is clearly observable by ITC. Therefore, if the initial binding of the incoming nucleotide can equally happen with nevirapine bound to the RT/DNA complex, this should also appear with ITC. However, we observed that only a rather small fraction of the complex was able to bind the incoming nucleotide (Figures S18 and S19). Our interpretation is that the bound nevirapine prevents initial binding of the incoming nucleotide and that the residual signal can be attributed to the residual fraction of RT/DNA complex that is not bound to nevirapine (Figure S19).

In order to test whether the order of addition of the DNA and of the nevirapine substrates could be significant, initial binding of the incoming dNTP was also investigated by incremental-ITC after preincubation of RT/NNRTI, followed by addition of DNA primer-template during a first ITC titration. As seen previously (Figure 5a,b), the addition of DNA to RT/NNRTI complex implies the formation of two distinct RT/NNRTI/DNA complexes. Again, no signal could be observed after addition of the incoming nucleotide (ddTTP or dTTP), neither for RT/DNA/nevirapine, nor for RT/DNA/efavirenz complexes (Figures 5 and S17), showing that in presence of these non-nucleoside inhibitors, the RT/DNA complex does not bind the nucleotide substrate.

■ DISCUSSION

Here we dissected thermodynamics of the mechanism of nucleotide incorporation by RT using a novel 'incremental-ITC' strategy. This approach is well-suited for the study of successive chemical reactions, such as nucleic acid polymerization by DNA- or RNA-polymerases. Two requirements, however, are to be fulfilled for a successful experimental framework: (i) the starting concentration of compound in the cell should be sufficient to ensure good data quality in the subsequent experiments and (ii) there should be no significant competition between the ligands added successively. As observed from single molecule studies,[11,12,18] our thermodynamic data also show that RT can adopt two binding modes on a nucleic acid primer-template, only one being able to bind incoming dNTP and thus corresponding to a DNA-polymerization competent orientation. The second orientation does not bind the incoming dNTP and is therefore nonproductive

dx.doi.org/10.1021/ja4018418 | J. Am. Chem. Soc. 2013, 135, 9743−9752

(Figures S2 and S3). The population of each binding mode strongly depends on the primer-template sequence and length.

Complete nucleotide incorporation can be modeled as a three step process: initial binding, chemical reaction, and translocation. Thermodynamics of the two last steps (which cannot be dissociated in a simple way) could be obtained by subtracting thermodynamic data for the initial binding of dNTP in absence of nucleotide incorporation from the complete DNA incorporation process. We showed that dNTP binding is mostly enthalpy driven but with significant differences between various nucleotides (−20.8 to −9.7 kcal·mol^{-1} at 25 °C). The enthalpy change following the chemical plus the translocation steps also depends on the nucleotide: it is poorly exothermic for dCTP and dGTP, but extrapolation of ITC data at 37 °C indicates that it might be endothermic at physiological temperature for dATP and dTTP (Figure 3). Since the chemical step is expected to be the same for all dNTPs, this difference likely relies on the translocation step. In this frame, the role of the sequence context remains to be tested. Furthermore, the use of compounds inhibiting the translocation step[41] might be useful to isolate the thermodynamic contribution of the translocation from that of the chemical reaction in DNA elongation.

Our data also show that dNTP binding to the polymerization-competent RT/DNA complex provides a significant amount of the free-energy change required for catalysis, with ΔG ranging from −7.5 to −9.0 kcal·mol^{-1}. As previously suggested, this energy produced by dNTP binding might be stored in a displacement of the conserved $Y_{183}MDD_{186}$ motif so that it can be later released during the translocation step.[42] In contrast, ITC data show that events including the chemical step and the RT translocation are only poorly exergonic for dATP, dTTP, and dCTP and endergonic for dGTP (Figure 3). Since the hydrolysis of dNTP produced during the chemical step is highly exergonic and provides about −10.9 kcal·mol^{-1} of free-energy change,[43] our data show that incoming nucleotide binding is a major driving force for DNA polymerization. This is in agreement with the observation that the conformational change involving closure of the p66 finger domain on the active site is the rate-limiting step in single nucleotide incorporation experiments.[25,33]

Previous kinetic analysis suggested that binding of NNRTI interferes with the chemical step of DNA polymerization but would not directly prevent binding of the incoming dNTP.[7−9] However, in a recent crystal structure of a cross-linked RT/DNA complex bound to nevirapine, grown in presence of AZTTP as an incoming nucleotide, the latter could not be observed in electron density maps.[10] This structure indeed shows that the dNTP binding site is highly distorted by the presence of nevirapine, shifting the 3′-hydroxyl of the DNA primer by more than 5 Å away from the polymerase active site, thus preventing a binding of the dNTP as observed in the RT/DNA/dNTP complex.[30] Moreover, smFRET studies have shown that NNRTI binding to the RT destabilizes the polymerization-competent binding of the enzyme to the DNA primer-template in favor of the RNaseH-active orientation.[11,12]

Thermodynamic data provided by the present study make a perfect bridge between these studies, clarifying the NNRTI inhibition mechanism. Two NNRTI inhibition pathways should be discerned. The first one (in blue in Figure 6) involves the binding of RT to the DNA primer-template first (characterized by ΔH_1 and ΔS_1), followed by the binding of NNRTI (ΔH_4, ΔS_4). The second pathway (in red in Figure 6) requires first binding of NNRTI to the apo-RT (ΔH_2, ΔS_2) and subsequent binding of DNA (binding mode 1 with ΔH_3, ΔS_3 and binding mode 2 with $\Delta H_{3'}$, $\Delta S_{3'}$). The presence of NNRTI alters the binding of RT on the DNA primer-template, resulting in a destabilization of the polymerization-competent orientation of the RT onto the DNA in favor of an opposite orientation unable to bind the incoming dNTP[11,12,18,44] (dead-end complex in Figure 6). Because the second binding mode is characterized by a thermodynamic signature quite different from the first one, it likely corresponds to a structure significantly different from catalytically competent RT/DNA complexes reported by X-ray crystallography. Finally, our data, obtained using a direct and label-free assay, showed that none of the binding modes of RT/NNRTI on the DNA primer-template are able to bind incoming dNTP (Figures 5 and S17), in contradiction with previous kinetic studies. Likely, the dNTP binding and the slow DNA polymerization observed in these studies in presence of NNRTI were due to the activity of a remaining fraction of free RT not bound to the inhibitor.

Analysis of the thermodynamics for both NNRTI inhibition pathways shows that the second pathway involving ΔH_3 and ΔS_3 (binding mode 1 in Table 2) is analogous to the first pathway ($\Delta H_1 + \Delta H_4 \sim \Delta H_2 + \Delta H_3$ and $T\Delta S_1 + T\Delta S_4 \sim T\Delta S_2 + T\Delta S_3$). In contrast, the pathway involving $\Delta H_{3'}$ and $\Delta S_{3'}$ (binding mode 2 in Table 2) leads to a different final state. Consequently, binding mode 1 can be assigned to the polymerization-competent orientation of RT on the DNA primer-template and binding mode 2 to the dead-end complex (Figure 6). Since the latter conformation is characterized by a 10-fold tighter affinity (Table 2), RT should preferentially interact through this binding mode with DNA when bound to a NNRTI. Furthermore, because the kinetics of NNRTI association with the catalytically competent RT/DNA complex is very slow compared to dNTP binding, and since NNRTI is not able to bind the RT/DNA/dNTP complex, our results strongly suggest, in line with an earlier report,[45] that a polymerizing elongation complex might be little susceptible to inhibition. As a consequence, RT should be targeted preferentially by NNRTIs as a free protein rather than bound to DNA.

■ CONCLUSION

In conclusion, our thermodynamic analysis of RT/NNRTI interactions suggests that NNRTI inhibition is mainly due to the binding of the inhibitor to the free RT, thus preventing a correct binding of RT to the DNA in a catalytically competent manner and leading to the formation of dead-end RT/DNA/NNRTI complexes that are unable to bind the incoming nucleotide substrate. Further thermodynamic studies of RT bound to viral RNA and to cellular $tRNA^{Lys}_3$ will be needed to clarify the role of NNRTIs during the initiation of reverse transcription.

■ MATERIALS AND METHODS

Sample Preparation. The RT (HIV-1, BH10 isolate) was expressed and purified as described previously.[46] The protein was then stored as a suspension in a 2 M $(NH_4)_2SO_4$ solution. Nevirapine and efavirenz were obtained through the NIH AIDS Research and Reference Reagent Program, Division AIDS, NIAID, NIH and were both dissolved in DMSO. The sequences of SeqB RNA and DNA primers are the same as that used in a previous smFRET study.[11] SeqB DNA template is a slightly shorter version of the SeqB DNA template

dx.doi.org/10.1021/ja4018418 | J. Am. Chem. Soc. 2013, 135, 9743−9752

according to the reference 11. Unmodified DNA and RNA sequences were purchased from Integrated DNA Technologies, purified by HPLC on a Dionex Nucleopac PA-100 by HPLC, and stored into water.

RT/DNA Cross-Linking. RT construct Q258C was expressed and purified as described.[35] The 20-mer primer DNA (5′ ACAGTCCCTGTTCGGGCGCC 3′) bearing a cross-linkable modified guanine was synthesized as described in the Supporting Information.

ITC. ITC measurements were performed on a MicroCal ITC200 (GE Healthcare) in R1 buffer (Mes-NaOH 10 mM, pH 6.5, NaCl 100 mM, $MgCl_2$ 2 mM). DMSO (0.8−1.8%) was added to the buffer in experiments involving nevirapine and efavirenz. ITC data were analyzed using the dedicated software by Microcal (Origin 7.0) and homemade software (written with Mathematica, Wolfram Research) for all aspects linked to 'global thermodynamic treatment' and kinITC. All data with dNTP addition were fitted with a single binding site model, except data with dGTP where two independent binding sites were used (one specific binding site and a weak unspecific binding site). Global thermodynamic treatment and kinITC analysis were performed as described.[24] For incremental-ITC experiments, after addition of 20−40 μL of the first substrate (DNA primer-template) into the RT (280 μL loaded in the sample cell), the syringe was washed and loaded with the first incoming nucleotide without removing RT/DNA sample from the cell. The cell concentration for the second experiment was adjusted to the concentration of the RT/DNA complex. Starting from the third incremental-ITC experiment, 40 μL of the elongated-RT/DNA complex was removed from the cell prior the experiment. The syringe was washed and loaded with the second incoming nucleotide, and the concentration in the cell was set to the concentration of elongated RT/DNA+1 complex. Blanks were performed by injecting the various ligands used (dNTPs, ddNTPs, nucleic acids, or NNRTIs) into buffer in order to subtract the heat of dilution from the reaction heat data.

■ ASSOCIATED CONTENT

Ⓢ Supporting Information

ITC profiles, thermodynamic data for dNTP binding, description of the chemical synthesis of the cross-linkable modified guanine, and methods for mass spectrometry analysis. This material is available free of charge via the Internet at http://pubs.acs.org.

■ AUTHOR INFORMATION

Corresponding Author

e.ennifar@ibmc-cnrs.unistra.fr

Present Addresses

[§]Swiss Group for Clinical Cancer Research (SAKK), Bern, Switzerland

[∥]Roche Diagnostics GmbH, Penzberg, Germany

Author Contributions

[⊥]These authors contributed equally.

Notes

The authors declare no competing financial interest.

■ ACKNOWLEDGMENTS

We are grateful to Dr. Stephen H. Hughes (NCI-Frederick) for providing the Q258C RT construct and to Dr. Redmond Smyth for critical reading of the manuscript. This project was supported by the 'Agence Nationale de Recherche sur le SIDA' (ANRS) and the Austrian Science Fund FWF (P21641 to R.M.). M.A.G. was supported by an ANRS postdoctoral fellowship. The following reagents were obtained through the NIH AIDS Research and Reference Reagent Program, Division AIDS, NIAID, NIH: nevirapine, efavirenz.

■ REFERENCES

(1) Jacobo-Molina, A.; Ding, J.; Nanni, R. G.; Clark, A. D., Jr.; Lu, X.; Tantillo, C.; Williams, R. L.; Kamer, G.; Ferris, A. L.; Clark, P.; et al. *Proc. Natl. Acad. Sci. U.S A.* **1993**, *90*, 6320.

(2) Kohlstaedt, L. A.; Wang, J.; Friedman, J. M.; Rice, P. A.; Steitz, T. A. *Science* **1992**, *256*, 1783.

(3) Das, K.; Bauman, J. D.; Clark, A. D., Jr.; Frenkel, Y. V.; Lewi, P. J.; Shatkin, A. J.; Hughes, S. H.; Arnold, E. *Proc. Natl. Acad. Sci. U.S A.* **2008**, *105*, 1466.

(4) Das, K.; Clark, A. D., Jr.; Lewi, P. J.; Heeres, J.; De Jonge, M. R.; Koymans, L. M.; Vinkers, H. M.; Daeyaert, F.; Ludovici, D. W.; Kukla, M. J.; De Corte, B.; Kavash, R. W.; Ho, C. Y.; Ye, H.; Lichtenstein, M. A.; Andries, K.; Pauwels, R.; De Bethune, M. P.; Boyer, P. L.; Clark, P.; Hughes, S. H.; Janssen, P. A.; Arnold, E. *J. Med. Chem.* **2004**, *47*, 2550.

(5) Ren, J.; Esnouf, R.; Hopkins, A.; Ross, C.; Jones, Y.; Stammers, D.; Stuart, D. *Structure* **1995**, *3*, 915.

(6) Smerdon, S. J.; Jager, J.; Wang, J.; Kohlstaedt, L. A.; Chirino, A. J.; Friedman, J. M.; Rice, P. A.; Steitz, T. A. *Proc. Natl. Acad. Sci. U.S A.* **1994**, *91*, 3911.

(7) Rittinger, K.; Divita, G.; Goody, R. S. *Proc. Natl. Acad. Sci. U.S A.* **1995**, *92*, 8046.

(8) Spence, R. A.; Kati, W. M.; Anderson, K. S.; Johnson, K. A. *Science* **1995**, *267*, 988.

(9) Xia, Q.; Radzio, J.; Anderson, K. S.; Sluis-Cremer, N. *Protein Sci.* **2007**, *16*, 1728.

(10) Das, K.; Martinez, S. E.; Bauman, J. D.; Arnold, E. *Nat. Struct. Mol. Biol.* **2012**, *19*, 253.

(11) Abbondanzieri, E. A.; Bokinsky, G.; Rausch, J. W.; Zhang, J. X.; Le Grice, S. F.; Zhuang, X. *Nature* **2008**, *453*, 184.

(12) Liu, S.; Abbondanzieri, E. A.; Rausch, J. W.; Le Grice, S. F.; Zhuang, X. *Science* **2008**, *322*, 1092.

(13) Geitmann, M.; Unge, T.; Danielson, U. H. *J. Med. Chem.* **2006**, *49*, 2375.

(14) Geitmann, M.; Unge, T.; Danielson, U. H. *J. Med. Chem.* **2006**, *49*, 2367.

(15) Gorshkova, II; Rausch, J. W.; Le Grice, S. F.; Crouch, R. *J. Anal. Biochem.* **2001**, *291*, 198.

(16) Radi, M.; Maga, G.; Alongi, M.; Angeli, L.; Samuele, A.; Zanoli, S.; Bellucci, L.; Tafi, A.; Casaluce, G.; Giorgi, G.; Armand-Ugon, M.; Gonzalez, E.; Este, J. A.; Baltzinger, M.; Bec, G.; Dumas, P.; Ennifar, E.; Botta, M. *J. Med. Chem.* **2009**, *52*, 840.

(17) Liu, S.; Harada, B. T.; Miller, J. T.; Le Grice, S. F.; Zhuang, X. *Nat. Struct. Mol. Biol.* **2010**, *17*, 1453.

(18) Rothwell, P. J.; Berger, S.; Kensch, O.; Felekyan, S.; Antonik, M.; Wohrl, B. M.; Restle, T.; Goody, R. S.; Seidel, C. A. *Proc. Natl. Acad. Sci. U.S A.* **2003**, *100*, 1655.

(19) Kvaratskhelia, M.; Miller, J. T.; Budihas, S. R.; Pannell, L. K.; Le Grice, S. F. *Proc. Natl. Acad. Sci. U.S A.* **2002**, *99*, 15988.

(20) Feig, A. L. *Biopolymers* **2007**, *87*, 293.

(21) Leavitt, S.; Freire, E. *Curr. Opin. Struct. Biol.* **2001**, *11*, 560.

(22) Privalov, P. L.; Dragan, A. I. *Biophys Chem* **2007**, *126*, 16.

(23) Velazquez Campoy, A.; Freire, E. *Biophys. Chem.* **2005**, *115*, 115.

(24) Burnouf, D.; Ennifar, E.; Guedich, S.; Puffer, B.; Hoffmann, G.; Bec, G.; Disdier, F.; Baltzinger, M.; Dumas, P. *J. Am. Chem. Soc.* **2012**, *134*, 559.

(25) Kati, W. M.; Johnson, K. A.; Jerva, L. F.; Anderson, K. S. *J. Biol. Chem.* **1992**, *267*, 25988.

(26) Schuckmann, M. M.; Marchand, B.; Hachiya, A.; Kodama, E. N.; Kirby, K. A.; Singh, K.; Sarafianos, S. G. *J. Biol. Chem.* **2010**, *285*, 38700.

(27) Manning, G. S. *Q. Rev. Biophys.* **1978**, *11*, 179.

(28) Datta, K.; LiCata, V. J. *Nucleic Acids Res.* **2003**, *31*, 5590.

(29) Datta, K.; Wowor, A. J.; Richard, A. J.; LiCata, V. J. *Biophys. J.* **2006**, *90*, 1739.

(30) Huang, H.; Chopra, R.; Verdine, G. L.; Harrison, S. C. *Science* **1998**, *282*, 1669.

(31) Spolar, R. S.; Record, M. T., Jr. *Science* **1994**, *263*, 777.

(32) Krebs, R.; Immendorfer, U.; Thrall, S. H.; Wohrl, B. M.; Goody, R. S. *Biochemistry* **1997**, *36*, 10292.

(33) Reardon, J. E. *Biochemistry* **1992**, *31*, 4473.
(34) Minetti, C. A.; Remeta, D. P.; Miller, H.; Gelfand, C. A.; Plum, G. E.; Grollman, A. P.; Breslauer, K. J. *Proc. Natl. Acad. Sci. U.S A.* **2003**, *100*, 14719.
(35) Huang, H.; Harrison, S. C.; Verdine, G. L. *Chem Biol* **2000**, *7*, 355.
(36) Sarafianos, S. G.; Clark, A. D., Jr.; Tuske, S.; Squire, C. J.; Das, K.; Sheng, D.; Ilankumaran, P.; Ramesha, A. R.; Kroth, H.; Sayer, J. M.; Jerina, D. M.; Boyer, P. L.; Hughes, S. H.; Arnold, E. *J. Biol. Chem.* **2003**, *278*, 16280.
(37) Maga, G.; Amacker, M.; Ruel, N.; Hubscher, U.; Spadari, S. *J. Mol. Biol.* **1997**, *274*, 738.
(38) Sluis-Cremer, N.; Tachedjian, G. *Virus Res.* **2008**, *134*, 147.
(39) Sarafianos, S. G.; Das, K.; Ding, J.; Boyer, P. L.; Hughes, S. H.; Arnold, E. *Chem. Biol.* **1999**, *6*, R137.
(40) Palaniappan, C.; Fay, P. J.; Bambara, R. A. *J. Biol. Chem.* **1995**, *270*, 4861.
(41) Michailidis, E.; Marchand, B.; Kodama, E. N.; Singh, K.; Matsuoka, M.; Kirby, K. A.; Ryan, E. M.; Sawani, A. M.; Nagy, E.; Ashida, N.; Mitsuya, H.; Parniak, M. A.; Sarafianos, S. G. *J. Biol. Chem.* **2009**, *284*, 35681.
(42) Sarafianos, S. G.; Clark, A. D., Jr.; Das, K.; Tuske, S.; Birktoft, J. J.; Ilankumaran, P.; Ramesha, A. R.; Sayer, J. M.; Jerina, D. M.; Boyer, P. L.; Hughes, S. H.; Arnold, E. *EMBO J.* **2002**, *21*, 6614.
(43) Frey, P. A.; Arabshahi, A. *Biochemistry* **1995**, *34*, 11307.
(44) Wohrl, B. M.; Krebs, R.; Goody, R. S.; Restle, T. *J. Mol. Biol.* **1999**, *292*, 333.
(45) Grobler, J. A.; Dornadula, G.; Rice, M. R.; Simcoe, A. L.; Hazuda, D. J.; Miller, M. D. *J. Biol. Chem.* **2007**, *282*, 8005.
(46) Freisz, S.; Bec, G.; Radi, M.; Wolff, P.; Crespan, E.; Angeli, L.; Dumas, P.; Maga, G.; Botta, M.; Ennifar, E. *Angew. Chem., Int. Ed. Engl.* **2010**, *49*, 1805.